Design Charts for Circular-Shaped Sheeted Excavation Pits against Seepage Failure by Heave

Serdar Koltuk, *Rafig* Azzam

Abstract

During the construction of an excavation pit, the main problem is often dominated by seepage flow into the excavation pit. The pore water pressure developed by the seepage flow may lift the excavation base, and thus, may lead to the stability loss of the excavation pit, which is known as seepage failure by heave. In this study, based on the results of three-dimensional steady-state groundwater flow analyses, design charts are given to evaluate the safety against heave of circular-shaped sheeted excavation pits constructed within homogeneous isotropic soil layers of limited or unlimited thicknesses. The given design charts consider the various conditions of water level on both up- and downstream side of an excavation pit. It means that they can be used for excavation pits constructed in both urban areas and open water.

Keywords

Circular-shaped sheeted excavation pits · seepage failure by heave · design charts

Serdar Koltuk

Department of Engineering Geology and Hydrogeology RWTH Aachen University Lochnerstr, 4-20, D-52064, Aachen, Germany
e-mail: koltuk@lih.rwth-aachen.de

Rafig Azzam

Department of Engineering Geology and Hydrogeology RWTH Aachen University Lochnerstr, 4-20, D-52064, Aachen, Germany
e-mail: azzam@lih.rwth-aachen.de

1 Introduction

Circular-shaped sheeted excavation pits are very common for the constructions of sewers, shafts, bridge piers and abutments. Due to appearing ring stresses, the earth pressure acting on the walls of a circular-shaped excavation pit is less than that in a square- or rectangular- shaped excavation pit. Therefore, they can be constructed without using struts or tie-back anchors, which reduces construction costs, and provides large working area.

After the construction of sheet piles, the water inside the excavation pit is pumped out which causes a reduction in both the pore water pressure and the total stress below the excavation base. Additionally, a further reduction of the total stress appears due to excavation processes. A seepage failure by heave occurs when the pore water pressure developed by the seepage flow overcomes the total pressure below the excavation base. As can be seen in Fig. 1a, the amount of soil deformations around the partition panel increases with increasing hydraulic head difference ΔH, and consequently, these deformations lead to the loss of the soil stability and/or the loss of the partition panel. For the verification against seepage failure by heave, various methods have been developed, the most well-known of which are mentioned below.

Terzaghi et al. determined from model tests that heave occurs within a distance of about D/2 from the partition panel (where D is the embedment depth of the partition panel), and the critical section passes through the base of the partition panel [1, 2]. Baumgart & Davidenkoff method, which has firstly presented in Russian language in 1929, considers the maximum pore water pressure that develops at the wall tip on the downstream side [3]. Harza stated that the exit hydraulic gradient on the downstream side is decisive with regard to heave [4]. Marsland identified two types of seepage failure through model tests: piping and heave. Piping occurs in dense sands when the exit hydraulic gradient adjacent to the partition panel becomes equal to critical hydraulic gradient of the soil whereas heave occurs in loose sands when the pore water pressure at the base of the partition panel becomes equal to the total stress at the same level [5]. Tanaka's failure concept, which is an extension of Terzaghi's

method, considers the frictional forces on the sides of various prismatic failure bodies adjacent to the sheet pile. The prism giving minimum factor of safety is decisive against heave [6].

For the case that a horizontal stratification exists between the excavation base and the wall tip, various verification methods against heave can also be found in the literature [2, 7, 8]. The present study focuses on the seepage failure by heave in homogeneous soil layers in which no horizontal stratification is present between the excavation base and the wall tip.
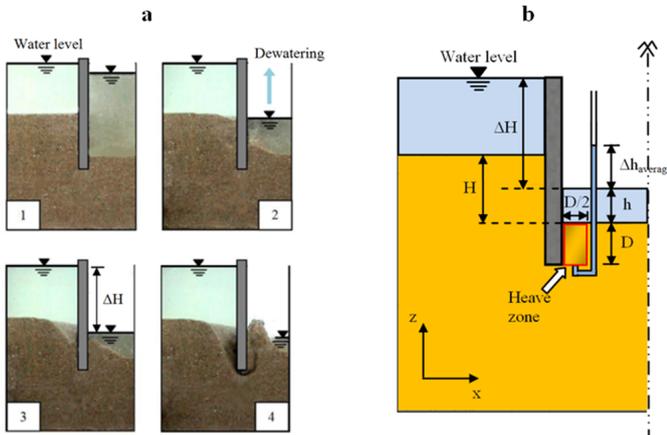
Fig. 1. Seepage failure by heave: a) development of heave in two-dimensional model tests, b) verification against heave

The most commonly used method to evaluate the safety against heave was introduced by Terzaghi et al. [2]. In his method, limit state condition is obtained by equating the average pore water pressure at the bottom of the heave zone with the construction-related total stress at the same level (see Fig. 1b):

$$h \cdot \gamma_w + D \cdot \gamma_{sat} = (\Delta h_{av} + h + D) \cdot \gamma_w \qquad (1)$$

Substituting ($\gamma_{sat} = \gamma' + \gamma_w$) into Eq. (1) gives

$$D \cdot \gamma' = \Delta h_{av} \cdot \gamma_w \qquad (2)$$

$$\frac{\gamma'}{\gamma_w} = \frac{\Delta h_{av}}{D} \qquad (3)$$

$$i_{cr} = i_{av} \qquad (4)$$

where γ_{sat} and γ' are the saturated and submerged unit weights of the soil respectively, γ_w is the unit weight of the water, Δh_{av} is the average hydraulic head at the bottom of the heave zone, h is the height of the water level on the excavation base, D is the embedment length of the wall below the water level, as shown in Fig. 1b. The ratios of $\Delta h_{av} / D$ and γ' / γ_w are called the average hydraulic gradient i_{av} and the critical hydraulic gradient of the soil i_{cr}, respectively.

The safety against heave is assured when i_{cr} is greater than i_{av}. However, the actual field conditions, namely the soil and the flow conditions, may differ from the assumed theoretical model. Therefore, the stability computations are only approximate and should be compensated using a safety factor (FS = i_{cr} / i_{av}). A

safety factor of 1.5 is recommended against seepage failure by heave [9]. But it is often uncertain whether the parts of embedded walls below the excavation base are 100% waterproof or not. In such cases, a higher safety factor should be used since a defect on the wall endangers the safety against seepage failure [10].

To determine the average hydraulic gradient i_{av} in the heave zone, the distribution of pore water pressure within the soil should be known. The theory of seepage flow through saturated soils is based on Laplace's equation, which is obtained by introducing Darcy's law into the continuity equation. Commonly, two-dimensional Laplace's partial differential equation is used to determine the distribution of pore water pressure within the soil:

$$k_x \cdot \frac{\partial^2 h}{\partial x^2} + k_z \cdot \frac{\partial^2 h}{\partial z^2} = 0 \qquad (5)$$

where k_x and k_z are the hydraulic conductivities of soil, $\partial h / \partial x$ and $\partial h / \partial z$ are the hydraulic gradients in any point within the soil in horizontal (x) and vertical (z) directions, respectively.

The solution of Eq. (5) is commonly obtained using a graph referred to as flow net. However, it is not easy to draw a flow net in complex flow conditions (e.g. in stratified soils), which is mostly the case in practical seepage problems. Furthermore, the experimental and numerical studies demonstrated that the pore water pressures obtained from three-dimensional models can be too larger than those obtained from two-dimensional models [6, 11–13].

In the present study, three-dimensional Laplace's partial differential equation is solved by using the finite element software ABAQUS 6.12 [14]. Based on the results of three-dimensional steady-state groundwater flow analyses, which also correspond to axisymmetric analyses, design charts are given. The charts enable users to evaluate the stability against heave of circular-shaped sheeted excavation pits constructed in homogeneous isotropic soil layers of limited or unlimited thicknesses.

2 Numerical Analyses

The numerical models used in this study consider only a quarter of circular-shaped sheeted excavation pits taking advantage of symmetry. The horizontal distance from the wall to the outer boundaries of the soil model R is chosen such that its effect on the results is negligibly small whereas the vertical distance from the wall base to the top surface of the lower soil layer T is varied between $0.0625 \cdot D$ and $8 D$ (see Fig. 2a). The thickness of the lower soil layer is chosen such that its effect on the hydraulic gradient is negligibly small. The water levels on the up- and downstream sides, which are shown with the blue-colored surfaces, lie on the top surface of the upper soil layer and on the excavation base, respectively. The symbol H in Fig. 2b represents the vertical distance between the level on the upstream side, where the water begins to flow through the soil, and the level on the downstream side, where the water flows out of the

soil. The symbols D and b represent the embedment length of the wall below the water level, and the radius of the excavation pit respectively.
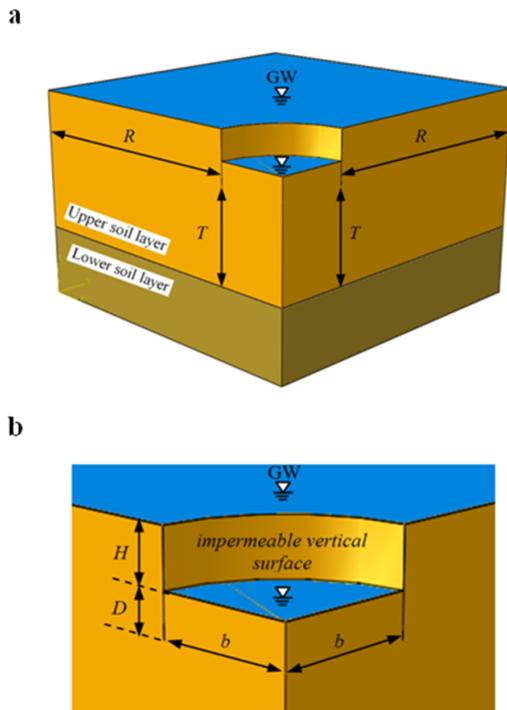
Fig. 2. Numerical model: (a) entire model; (b) zoom of the excavation pit

The sheet piles are modelled using a gap with an ignorable thickness. The surfaces of the sheet piles are impermeable by default. The vertical boundaries and the bottom boundary of the soil models are also impermeable. The deformations of the models that result from the groundwater flow, in other words from the change of effective stresses, are prevented. The soil layers are modelled with 8-node brick trilinear displacement/pore pressure elements (C3D8P). The mesh is refined near the wall where the flow gradients are concentrated. The number of elements in the models is chosen such that its effect on the results is negligibly small. Accordingly, the number of elements varies between about 20,000 and 100,000 depending on the model size. The water level on the downstream side, namely the level of the excavation base is considered as reference level. Accordingly, the pore pressure boundary condition on the upstream side is set equal to the potential head H, and on the downstream side is set equal to zero.

3 Results and Discussions

In the given design charts, it is distinguished between two basic cases: In the first case, the upper soil layer is assumed to be more permeable than the lower soil layer $k_{upper}/k_{lower} > 1$ while the lower layer is assumed to be more permeable than the upper layer $k_{upper}/k_{lower} < 1$ in the second case. Accordingly, the ratio of k_{upper}/k_{lower} varied as $100/1$, $10/1$, $2.5/1$ and $1/2.5$, $1/10$, $1/100$. The numerical investigations have shown that the ratios of k_{upper}/k_{lower} greater than $100/1$ or less than $1/100$ have no considerable effect on the average hydraulic gradient i_{av} when

compared to the cases of $k_{upper}/k_{lower} = 100/1$ or $1/100$, respectively.
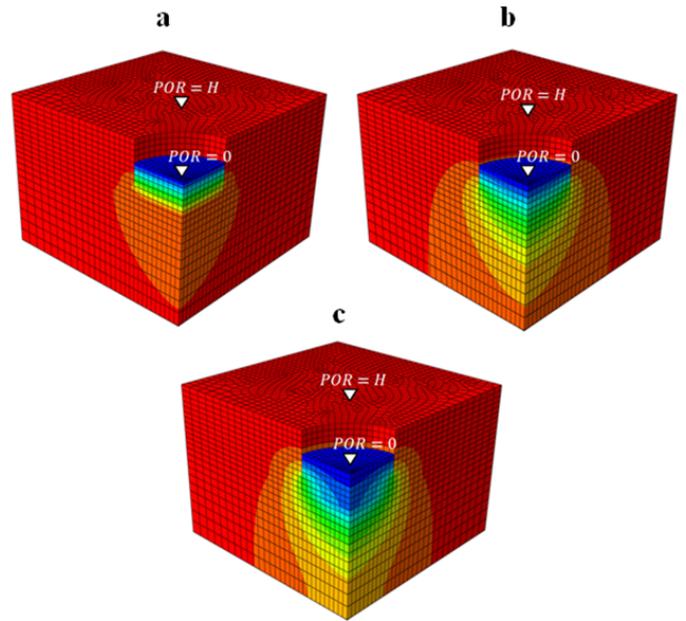
Fig. 3. Equipotential lines (surfaces): (a) $k_{upper}/k_{lower} < 1$, (b) $k_{upper}/k_{lower} = 1$, (c) $k_{upper}/k_{lower} > 1$
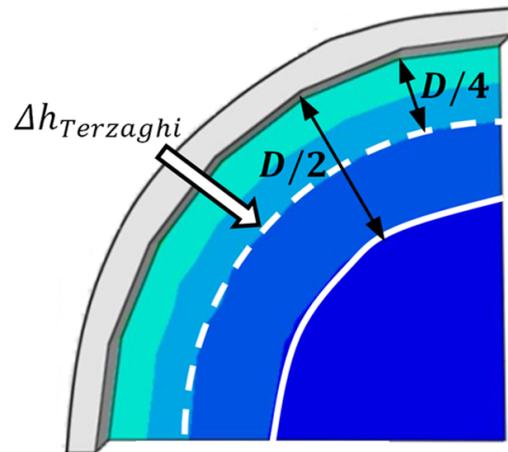
Fig. 4. Base of the assumed three-dimensional failure body

Fig. 3 shows the equipotential lines (surfaces) for circular-shaped sheeted excavation pits constructed within homogeneous soil layers of limited ($k_{upper}/k_{lower} \neq 1$) and unlimited thicknesses ($k_{upper}/k_{lower} = 1$). In the case of $k_{upper}/k_{lower} < 1$, most of the potential drops take place in the upper soil layer, as shown in Fig. 3a. As a result, the average hydraulic gradient in the failure body becomes greater than that in homogeneous soil layer of unlimited thickness (see Fig. 3b). On the other hand, i_{av} occurring in the homogeneous soil layer of unlimited thickness is greater than that in the case of $k_{upper}/k_{lower} > 1$ (see Fig. 3c).

A three-dimensional body with the width suggested by Terzaghi for two-dimensional cases is considered as failure body. The white-colored dashed line with a distance of $D/4$ from the wall in Fig. 4 indicates the location of the average pore water pressure at the bottom of the failure body.
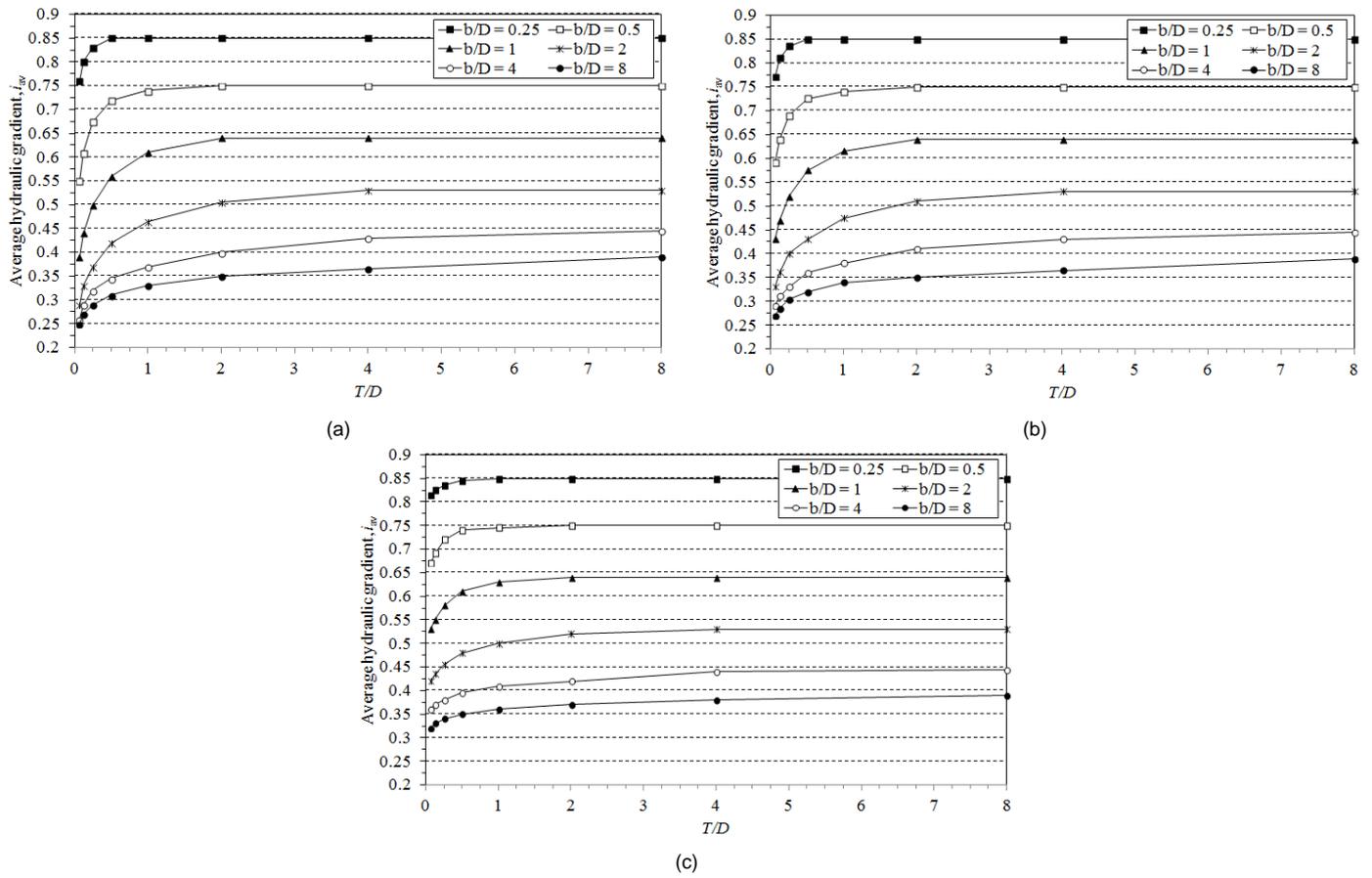
Fig. 5. Design charts against seepage failure by heave in the case of k_{upper}/k_{lower}: a) 100/1, b) 10/1, c) 2.5/1
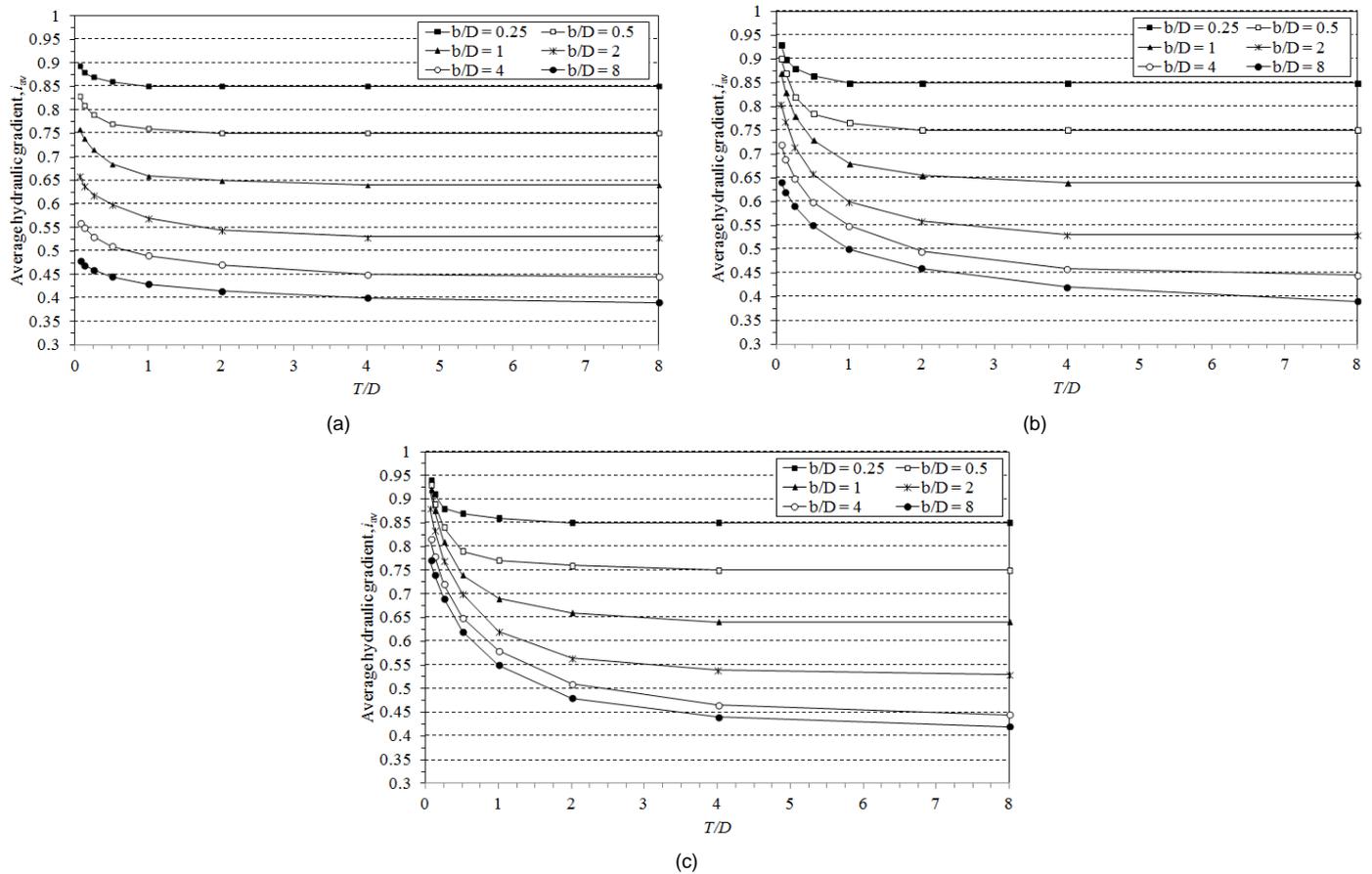
Fig. 6. Design charts against seepage failure by heave in the case of k_{upper}/k_{lower}: a) 1/2.5, b) 1/10, c) 1/100

In Fig. 5 and Fig. 6, the design charts are given to evaluate the safety against heave of circular-shaped sheeted excavation pits. In the charts, the average hydraulic gradients were determined for six various ratios of $b/D = 0.25, 0.5, 1, 2, 4, 8$ and eight various ratios of $T/D = 0.625, 0.125, 0.25, 0.5, 1, 2, 4, 8$. For other ratios of b/D and T/D that lying between the values given above, i_{av} can be determined using a linear interpolation. As can be seen in Figs. 5 and 6, the lower soil layer loses its effect on the average hydraulic gradient developed in the failure body for the ratios of T/D above a certain value depending on the ratio of b/D. In this case, the upper soil layer can be assumed as a homogeneous isotropic soil layer of unlimited thickness. Accordingly, all charts give the same value of i_{av} for a same ratio of b/D.

It should be mentioned that:

1 the given design charts are valid for $H/D = 1$. In order to determine the average hydraulic gradient i_{av} for the other ratios of H/D, the values of i_{av} obtained from the charts must be multiplied by H/D. In the case that H is equal to zero, the values of i_{av} obtained from the charts must be multiplied by the ratio of potential difference to embedment depth $\Delta H/D$. An average hydraulic gradient that is obtained in this way contains a maximum error of $\pm 5\%$;

2 the given design charts are valid for excavation pits, which correspond to the case in Fig. 7a. When the water level on the downstream side lies above the excavation base and/or the water level on the upstream side lies above the ground surface, the average hydraulic gradient i_{av} obtained from Fig. 5 or Fig. 6 must be multiplied by $\Delta H/H$. The symbols ΔH, H are shown in Fig. 7 for the various conditions of the water level;
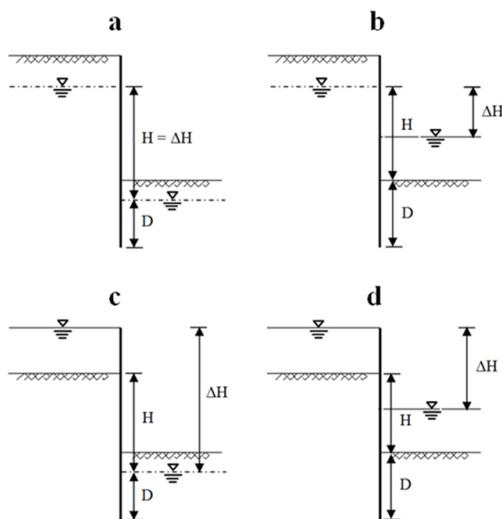
Fig. 7. Use of the given charts for various water level conditions

3 Equation (3), $i_{cr} = \gamma'/\gamma_w$, is valid when the groundwater level on the downstream side lies on or above the excavation base. If the groundwater level is kept below the excavation base for safety reasons, the critical hydraulic gradient i_{cr} is given as:

$$i_{cr} = \frac{d \cdot \gamma + D(\gamma_{sat} - \gamma_w)}{D \cdot \gamma_w} \qquad (6)$$

where γ is the moisture unit weight of soil, d is the distance between the excavation base and the pumped groundwater level on the downstream side, and D is the embedment length of the wall below the pumped groundwater level (see Figures 7a and 7c).

In the following, the use of the given design charts is explained through two examples. For this purpose, a circular-shaped sheeted excavation pit with the dimensions given in Fig. 8 is examined first.

The excavation pit is constructed within a silty fine sand, which is underlain by a gravelly sand with a permeability coefficient of 4.5×10^{-4} m/s, in an urban area. The silty fine sand has a permeability coefficient of 5×10^{-6} m/s. The moisture and saturated unit weights of the silty fine sand are 19 and 19.5 kN/m³ respectively. The unit weight of water is assumed to be 10 kN/m³.

From Fig. 8, the ratios of H/D, b/D and T/D are determined as $8/4 = 2$, $4/4 = 1$, $2/4 = 0.5$ respectively. The ratio of k_{upper}/k_{lower} is equal to $1/90$, so that the average hydraulic gradient i_{av} is determined as 0.74 from Fig. 6c. But this value is valid for $H/D = 1$, so that it must be multiplied by $H/D = 2$. Finally, i_{av} is calculated as $0.74 \times 2 = 1.48$.

The critical hydraulic gradient is calculated by Eq. (6):

$$i_{cr} = \frac{0.5 \times 19 + 4 \times (19.5 - 10)}{4 \times 10} = 1.19$$

Then the safety factor is calculated as:

$$FS = \frac{i_{cr}}{i_{av}} = \frac{1.19}{1.48} = 0.8$$
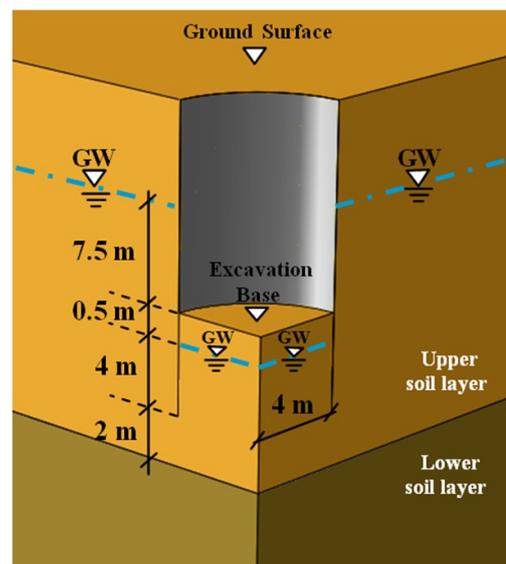
Fig. 8. A model example to use of the given design charts for circular-shaped excavation pits in urban areas

In the second example, a circular-shaped sheeted excavation pit with the dimensions given in Fig. 9 is studied. The excavation pit is constructed within a gravely sand, which is underlain by a cohesive soil with a permeability coefficient of 1.25×10^{-8} m/s, in open water. The gravely sand has a permeability coefficient of 2×10^{-6} m/s and a saturated unit weight of 20 kN/m^3. The unit weight of water is assumed to be 10 kN/m^3.
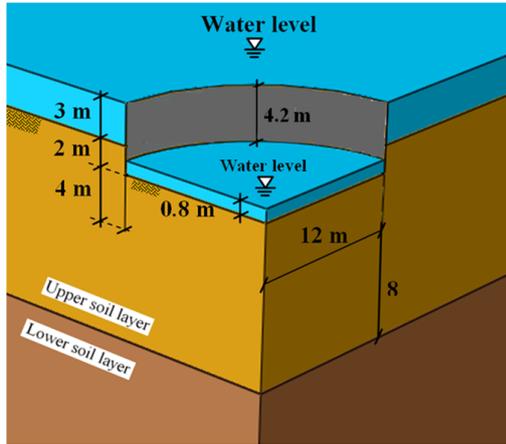
Fig. 9. A model example to use of the given design charts for circular-shaped excavation pits in open water

From Fig. 9, the ratios of H/D, b/D and T/D are determined as $2/4 = 0.5$, $12/4 = 3$, $8/4 = 2$, respectively. The ratio of k_{upper}/k_{lower} is equal to 160, so that the average hydraulic gradient i_{av} is determined as 0.45 from Fig. 5a. But this value is valid for $H/D = 1$, so that it must be multiplied by $H/D = 0.5$. Furthermore, the values obtained from the given design charts are valid for excavation pits, which correspond to the case in Fig. 7a. However, the water level conditions in this example correspond to the case in Fig. 7d, so that the determined value must also be multiplied by $\Delta H/H = 4.2/2 = 2.1$. Finally, i_{av} is calculated as $0.45 \times 0.5 \times 2.1 = 0.47$.

The critical hydraulic gradient is calculated by Eq. (3):

$$i_{cr} = \frac{\gamma_{sat} - \gamma_w}{\gamma_w} = \frac{20 - 10}{10} = 1$$

Then the safety factor is calculated as:

$$FS = \frac{i_{cr}}{i_{av}} = \frac{1}{0.47} = 2.1$$

4 Conclusions

The average hydraulic gradients on the downstream sides of circular-shaped sheeted excavation pits with various dimensions are determined, and the results are presented in the form of charts. Utilizing the given charts, the safety factor against heave of circular-shaped sheeted excavation pits, which are constructed within homogeneous isotropic soil layers of limited or unlimited thicknesses in open water or urban areas, can be easily and quickly evaluated.

References

1 **Terzaghi K**, *Erdbaumechanik auf bodenphysikalischer Grundlage*, Franz Deuticke-Verlag; Leipzig/Wien, 1925.

2 **Terzaghi K, Peck RB**, *Soil mechanics in engineering practice*, John Wiley & Sons; New York, 1968.

3 *EAU, Recommendations of the committee for waterfront structures, harbours and waterways*; Berlin, 2012.

4 **Harza LF**, *Uplift and seepage under dams in sand*, Transactions of the American Society of Civil Engineering, **100**(1), (1935), 1352–1385.

5 **Marsland A**, *Model experiments to study the influence of seepage on the stability of a sheeted excavation in sand*, Géotechnique, **3**(6), (1953), 223–241.

6 **Tanaka T, Song S, Shiba Y, Kusumi S, Inoue K**, *Seepage failure of sand in three dimensions-experiments and numerical analyses*, 6th International Conference on Scour and Erosion, (August 27-31, 2012), `http://scour-and-erosion.baw.de/icse6-cd/data/articles/000144.pdf`.

7 **Schober P, Boley C**, *Der Einfluss eines Auflastfilters auf den Bruchvorgang beim hydraulischen Versagen nichtbindiger Böden*, Geotechnik, **37**(4), (2014), 250–258. (in German).

8 **Pane V, Cecconi M, Napoli P**, *Hydraulic heave failure in EC7: Suggestions for Verification*, Geotechnical and Geological Engineering, **33**(3), (2015), 739–750, DOI 10.1007/s10706-014-9834-8.

9 *EN 1997-1: Eurocode 7, Geotechnical design-Part 1: General rules*, European Committee for Standardisation; Brussels, 2004.

10 **Ahmed Ashraf A, Johnston HT, Oyedele L**, *Hydraulic structures with defective sheet pile walls*, Dams and Reservoirs, **23**(1), (2013), 29–37, DOI 10.1680/dare.13.00017.

11 **Cai F, Ugai K, Takahashi C, Nakamura H, Okaki I**, *Seepage analysis of two case histories of piping induced by excavations in cohesionless soils*, The first International Conference on Construction, (August 12-14, 2004), `www.forum8.co.jp/english/icci/ICCI2004-analysis.pdf`.

12 **Aulbach B, Ziegler M**, *Simplified design of excavation support and shafts for safety against hydraulic heave*, Geomechanics and Tunnelling, **6**(4), (2013), 362–374, DOI 10.1002/geot.201300031.

13 **Koltuk S, Fernandez-Steeger M, Azzam R**, *A numerical study on the seepage failure by heave in sheeted excavation pits*, Geomechanics and Engineering, **9**(4), (2015), 513–530, DOI 10.12989/gae.2015.9.4.513.

14 *Abaqus analysis user's manual*, Vol. Vol. 1-5, Hibbitt, Karlsson and Sorenson, Inc., 2012.